Diesel soot combustion with perovskite catalysts

Diesel soot combustion with A1-xA'xB1-yB'yO3±δ perovskite catalysts

Journal:	*Chemical Engineering Communications*
Manuscript ID:	GCEC-2012-0329.R2
Manuscript Type:	Short Communication
Date Submitted by the Author:	n/a
Complete List of Authors:	Bensaid, Samir; Politecnico di Torino, Blengini, Giovanni; Politecnico di Torino, Fino, Debora; Politecnico di Torino, Russo, Nunzio; Politecnico di Torino,
Keywords:	Air pollution control, Catalysis, Combustion, Kinetics, Nanoparticles, Oxidation, diesel engine, soot

DIESEL SOOT COMBUSTION WITH $A_{1-x}A'_xB_{1-y}B'_yO_{3\pm\delta}$ PEROVSKITE CATALYSTS

S. Bensaid[1], G. A. Blengini[2], D. Fino[1], N. Russo[1,*]

[1] *Department of Applied Science and Technology*

Politecnico di Torino, Corso Duca degli Abruzzi 24, 10129 Torino, Italy.

[2] *Department of Environment, Land and Infrastructures Engineering*

Politecnico di Torino, Corso Duca degli Abruzzi 24, 10129 Torino, Italy.

** corresponding author: tel./fax: +39-011-0904710/4699;*

e-mail: nunzio.russo@polito.it

Abstract

Diesel soot emissions from stationary or mobile sources can be reduced through physical trapping in particulate filters until periodical *in-situ* combustion takes place. This study focuses on the development of several perovskites for the catalytic combustion of diesel particulates in multifunctional catalytic reactors. Several perovskites, with BET surface areas of 20-30 m^2/g, were prepared by the solution combustion synthesis method and were characterized by XRD, SEM, TEM and TPD techniques. Catalytic activity tests have shown that the most promising catalysts, namely, perovskite catalysts with Cr in the B site and Tb or Pr in the A site, can ignite soot combustion well below 400°C, i.e., at a temperature 200-250°C lower than that of non-catalytic diesel soot combustion.

The best catalytic formulation was deposited on a full-scale wall-flow filter and tested against the soot emissions of a diesel engine, resulting in a reduced regeneration time and a substantial fuel consumption saving compared to the corresponding bare filter performance.

Keywords: perovskite catalysts, soot combustion, wall-flow traps, diesel engine, emissions.

1. Introduction

Pollution from diesel engines contributes a significant share of planetary air-quality problems due to the emission of nitrogen oxides and particulates. With the growing concern over health effects associated with diesel soot, the reduction in diesel particulate emissions from stationary and mobile sources has become a requirement in urban areas (Neumann, 2002; Ye et al., 1999). Diesel particulates belong to the family of particulates under 2 microns, the so called "lung-damaging dust" family, and can easily be inhaled by humans. Modern diesel engines emit soot particles with an average diameter of 100 nm (Caroca et al., 2011), which are widely recognized as carriers for a number of harmful substances, and many authors suggest that long-term exposure to this fine particulate matter is a risk factor for cardiovascular disease mortality (e.g. Pope et al., 2004).

A simple way to overcome the problem of diesel particulates is to combine a trap for filtration purposes with an oxidation catalyst (Pontikakis et al., 2001, Bensaid et al. 2010), which is deposited in the trap for regeneration purposes, through catalytic combustion of the trapped soot.

The phenomena involved in soot catalytic combustion are multi-scale and complex. At the filter scale (10^{-2}-10^{-3} m), the composition (Darcy et al., 2007) and distribution of soot in the filter channels (Bensaid et al., 2009a,b) plays a significant role in the propagation of the thermal front in the axial and radial directions during regeneration. At the meso-scale (10^{-5}-10^{-7} m), the boundary between the deposited soot cake and the catalytic layer defines the contact points at which effective soot oxidation occurs (Aneggi et al., 2012a), which could be enhanced by catalyst morphology optimization (e.g. Kumar et al., 2012). At the micro-scale (10^{-8}-10^{-9} m), the catalyst cluster size, crystalline structure (Fino et al., 2003a; Atribak et al., 2008) and composition are decisive in soot oxidation activity. In this regard, catalyst formulations that are able to undergo redox cycles are developed by increasing their defective crystalline structure or by exposing crystalline planes that are particularly active towards redox cycles (Aneggi et al., 2012b), as well as by enhancing the oxygen storage capacity of catalyst formulations to rapidly restore the oxidation state of the active

metal following soot oxidation. The composition and cluster size can also be tailored to promote indirect oxidation mechanisms, e.g., in the case of NO_2-mediated soot oxidation enabled by PGM catalysts.

This paper describes the research and development of new perovskite catalytic formulations $A_{1-x}A'_xB_{1-y}B'_yO_{3\pm\delta}$ for soot oxidation. Starting with $LaCrO_3$ (Russo et al., 2005), particular investigation has been dedicated to the role of partial or total substitution of La at the A site. The effects of replacing some of the La with lower valence alkali metals or with equivalent or higher valence rare earth metals are shown in terms of soot oxidation activity. In fact, the latter can be enhanced by facilitating the redox cycle of chromium through charge imbalances induced by the different valences of the La substituent or through the lower stability of the crystalline reticulum caused by the different ionic radii of the La substituents; both of these enhancements foster soot oxidation (Russo et al., 2005). Additionally, the storage and superficial mobility of oxygen increase the ability to deliver oxygen to the catalyst-soot interface. In particular, the synergism between Pr and Ce (Fino and Specchia, 2004; Krishna et al. 2007) in performing the above-mentioned functionalities was exploited through the partial substitution of La with both elements in the same perovskite structure to reach a stable and extremely active catalytic formulation towards soot oxidation. Moreover, the new perovskite catalysts developed in this work should be less expensive than the Pt-based catalysts currently employed in commercial applications.

2. Experimental

2.1 Catalyst synthesis

The combustion synthesis technique used for catalyst preparation involved phenomena and reactions that allow the process to be self-sustaining from an energetic viewpoint (Merzahanov, 1996; Civera et al., 2003). A homogeneous aqueous solution of metal nitrates and urea was placed into an oven at a constant temperature between 400°C and 800°C; it quickly began to boil and froth

until ignition took place. The general reaction scheme leading to the production of $PrCrO_3$ follows (the hydration of both praseodymium and chromium nitrates has been neglected):

$$Pr(NO_3)_3 + Cr(NO_3)_3 + 5\ CO(NH_2)_2 \rightarrow PrCrO_3 + 5\ CO_2 + 8\ N_2 + 10\ H_2O \quad (1)$$

The whole reaction can be regarded as the sum of two different contributions:

$$5\ CO(NH_2)_2 + 15/2\ O_2 \rightarrow 5\ CO_2 + 10\ H_2O + 5\ N_2 \quad (2)$$

$$Pr(NO_3)_3 + Cr(NO_3)_3 \rightarrow PrCrO_3 + 3\ N_2 + 15/2\ O_2 \quad (3)$$

The exothermic reaction (2), namely, urea combustion, provides the heat necessary for reaction (3), i.e., the endothermic transformation of nitrates into the desired oxide. The entire process lasts only a few minutes, and the result is an inorganic foam that crumbles easily and has a very high specific volume and surface area.

Metal nitrates are the best starting materials because they are highly soluble in water and act as an oxygen source during the reaction (see Eq. 1-3). In some cases, to obtain oxides with a larger specific area, additives might be required. These additives must generate large quantities of gas and must provide the reacting system with more oxygen. Among the different possibilities, NH_4NO_3 seemed to be the most promising because during decomposition (Eq. 4), it develops gaseous products that do not contaminate the oxide and provide the system with heat in addition to the heat from the oven.

$$NH_4NO_3 \rightarrow N_2 + 2\ H_2O + 1/2\ O_2 \quad (4)$$

Moreover, NH_4NO_3 is inexpensive and, like the other nitrates, brings more oxygen into the system. However, ammonium nitrate is an explosive compound, and the handling of this material at an industrial level might involve additional costs linked to process safety, which hinders its practical application.

2.2 Characterization

X-ray diffraction was performed on the fresh catalysts to verify that the desired perovskite structure was achieved. In all cases, the desired structure was verified.

The BET specific surface areas of the prepared catalysts were evaluated from the linear parts of the BET plot of the N_2 isotherms using a BET analyzer. The specific surface area of the bulk and non-porous catalysts was directly related to the average crystal size, which was directly observed by transmission electron microscopy (TEM). TEM was used to analyze the microstructure of the different catalyst powders in more detail.

Scanning electron microscopy (SEM) and energy dispersion spectroscopy (EDS) were conducted to investigate the catalyst morphologies and to check the elemental composition and distribution of the catalysts. An even element distribution was generally observed in these cases.

Oxygen desorption tests were performed on a selected sub-set of the perovskites to examine the nature and the specific quantity of the oxygen species released by the catalyst at different temperature values.

A TPD/R/O analyzer equipped with a thermal conductibility detector (TCD) was used. The procedure was as follows: a fixed bed of catalyst was enclosed in a quartz tube and sandwiched between two quartz wool layers; prior to each temperature-programmed desorption (TPD) run, the catalyst was heated under an O_2 flow (40 Nml/min) to 750 °C. After 30 min under an O_2 flow at 750°C, the reactor temperature was lowered to room temperature while maintaining the same oxygen flow rate, thereby allowing complete oxygen adsorption over the catalyst. Afterwards, helium was fed to the reactor at a 10 ml/min flow rate and maintained at room temperature for 1 h to purge any excess oxygen. The catalyst was then heated to 1100 °C at a constant rate of 10 °C/min under a helium flow rate of 10 ml/min. The O_2 desorbed during the heating was detected by the TCD detector.

2.3 Catalytic formulation development approach

Several developmental pathways were investigated to improve the intrinsic activity of $LaCrO_3$, which is a particularly promising perovskite due to its ability to chemisorb oxygen at moderate temperatures (300-400°C):

- use of substoichiometric amounts of Cr and partial substitution of La (valence: +3) with monovalent K (both procedures maximize the presence of high-valence chromium species and the oxygen-exchange properties of the perovskite);
- partial or total substitution of La with rare earth metals of valence +2/+3 such as Sm, Eu, Yb and Tm;
- partial or total substitution of La with rare earth metals of valence +3/+4 such as Ce, Tb and Pr;
- total substitution of La with other rare earth metals with the same fixed valence +3 such as Gd, Ho, Lu and Er.

2.4 Catalytic activity of powders

The catalytic activity of the prepared catalysts was tested in a temperature programmed combustion (TPC) apparatus with soot-catalyst mixtures (Figure 1). A detailed description of the TPC equipment has been reported in our previous papers (e.g. Bensaid et al., 2011). Air was fed at a constant rate of 100 ml/min into a fixed-bed micro reactor, corresponding to a GHSV of 30,000 h^{-1}, and sandwiched between two quartz wool layers. The fixed-bed consisted of approximately 50 mg of the soot-catalyst mixture (5 mg of soot and 45 mg of catalyst, i.e., 1:9 on a mass basis) in tight contact conditions, to which 200 mg of SiO_2 (0,2÷0,7 mm granulate) had previously been added to reduce pressure drops in the bed itself and to provide a thermal dilution to avoid severe temperature gradients. The silica particles (average diameter of 100 μm) prevented bed compaction and preferential paths formation, which otherwise would occur if only catalyst (<10 μm) and soot (<1 μm) particles were present. The experiments were performed using dry amorphous carbon (Printex U from Degussa) instead of real diesel soot because the amorphous carbon is more difficult to burn than the real diesel soot (a conservative condition) due to the absence of unburned hydrocarbons that are found in diesel particulates, which facilitate diesel soot combustion. Dry soot has the advantage of providing a consistent composition, structure and reactivity throughout the full set of experiments and ensures better reproducibility because it is not dependent on the ever-changing

diesel engine conditions that produce real diesel soot. The reaction temperature was controlled through a PID-regulated oven and was increased during a TPC run from 200 to 700°C at a rate of 5 °C/min. The analysis of the outlet reactor gas was performed using CO and CO_2 NDIR analyzers (CO_2 and CO precision of 10 ppm and 1 ppm, respectively). The conversion peak temperature was registered as an index of catalytic activity. Each catalytic test was repeated three times with fresh catalysts, and the resulting curves were averaged. The differences in peak temperatures were always less than 5°C.

The activation energy of soot combustion over the prepared catalysts was measured according to the Ozawa method (Ozawa, 1970; Ozawa, 1975) through an appropriate interpretation of the thermal analysis data obtained with the DSC apparatus (Perkin Elmer DSC-Pyris).

2.5 Full-scale activity of supported catalysts

A selected catalyst formulation was deposited on a full-scale wall-flow filter provided by Corning (cell structure: 14/200, diameter: 300 mm, length: 6–12"; average pore diameter: 9 μm, porosity: 42%), by means of the *in-situ combustion synthesis* (Fino et al., 2003b), in a specific amount of 10 wt% with respect to filter weight. The catalyzed trap were tested in a pilot plant described in Fino et al. (2003a) on real diesel exhaust gases (Kubota 1000 cm^3 IDI engine), where the temperature and gas composition before and after the trap could be controlled and monitored as well as the filtration efficiency and the evolution of the pressure drop through the trap (a sign of soot accumulation therein). The pressure drop across the trap was measured by means of differential pressure transducers (VIKA; precision: 1 mbar) whereas the trap inlet and outlet temperature was measured by K-type thermocouples (precision: 1K) at axial locations just ahead and after the trap. The trap was loaded by feeding it with exhaust gases until a pressure drop of about 250 mbar was reached (corresponding to a particulate hold-up of about 15 g/l). Afterwards, the regeneration was induced by post injecting for a fixed time period (e.g. 100 s) some fuel in the exhaust gases with a metering pump (post-injected fuel specific flow rate: 0.005–0.015 kg/kg of exhaust gases) and by

burning these HCs with an oxidizing honeycomb catalyst (OXICAT by Johnson Matthey) placed just upstream the trap. The time needed for a complete trap regeneration (e.g. combustion of the soot hold-up) was considered as an index of the catalyst performance.

3. Results and discussion

3.1 A site substitution effect on $LaCrO_3$

XRD analysis found the perovskite samples to be well crystallized (not reported here for the sake of brevity), and no secondary phases were detected. The EDS confirmed that in the different zones of the catalyst surface, the ratios between atoms in the A or A' site and the atoms in the B or B' site were constant and equal to the ratios of the original precursors.

Figure 2a shows a representative SEM image of a $TbCrO_3$ perovskite catalyst produced via combustion synthesis (Civera et al., 2003). The $TbCrO_3$ perovskite catalyst microstructure appears foamy. During combustion synthesis, the decomposition/combustion of reacting precursors generates a large quantity of gaseous product over a very short period, which leads to a spongy catalyst morphology. This feature can be considered a great advantage because it favors the formation of rough interfaces for the catalyst powder agglomerates, which intensifies the contact conditions between the catalyst and the accumulating soot.

The TEM image in Figure 2b, which is representative of the full set of synthesized catalysts, shows that most of the perovskite crystals have a size range between 10 and 20 nm. Moreover, this particle size is perfectly in line with the BET surface areas of the various prepared catalysts (approximately 20-30 m^2/g; see Table 1), which can be verified through the simple calculation of a single particle's surface over its weight (considering the bulk density of the given oxide) corrected for by a proper area shading factor due to particle-particle contact.

In previous papers (Fino et al. 2003a, Russo et al. 2005), we reported the superior catalytic activities of $LaCrO_3$ and $LaCr_{0.9}O_{3-\delta}$ perovskites, via temperature programmed oxidation/reduction studies, on the basis of the primary role of weakly suprafacial chemisorbed oxygen active species.

In the present paper, the possibility of improving the activity of these catalysts has been examined according to the procedures indicated in the previous section.

Three catalysts ($TbCrO_3$, $PrCrO_3$, $CeCrO_3$) showed superior soot catalytic combustion activity during the first phase of the screening tests (see Figure 3a). These materials were capable of igniting soot combustion well below 400°C. Unfortunately, most likely due to the higher thermal stability of CeO_2, after aging at a high temperature, the $CeCrO_3$ catalyst changed in morphology and composition until a stoichiometric mixture of CeO_2 and Cr_2O_3 formed (Palmisano, 2005).

Although $TbCrO_3$ showed a slightly better catalytic performance than $PrCrO_3$, the cost of terbium is much higher than the one of praseodymium (see current prices at www.chemicool.com), which offsets this advantage in practical applications.

For these reasons, further studies focused on $PrCrO_3$ are needed. Starting from $PrCrO_3$, different perovskites have been obtained by substitutions in the A site to obtain the best compromise between activity, thermal stability and precursor cost.

3.2 Ce promotion effect on $PrCrO_3$ perovskite

Figure 3b illustrates the second part of the screening where substituted perovskites were compared with CeO_2. Three optimal compositions can be observed: $Ce_{0.9}K_{0.1}CrO_3$, $Ce_{0.8}La_{0.2}CrO_3$ and $Ce_{0.5}Pr_{0.3}La_{0.2}CrO_3$. Only $Ce_{0.5}Pr_{0.3}La_{0.2}CrO_3$ displayed both suitable activity and acceptable stability of the perovskite structure after calcination. The perovskite structure of $Ce_{0.5}Pr_{0.3}La_{0.2}CrO_3$ was maintained without a segregation of phases such as La_2O_3, Cr_2O_3 or CeO_2, as was observed in the XRD comparison of $PrCrO_3$, $Pr_{0.9}Ce_{0.1}CrO_3$ and $Ce_{0.5}Pr_{0.3}La_{0.2}CrO_3$ in Figure 4, where a progressive reduction in the degree of crystallinity was observed with an increasing A site substitution and a preservation of the perovskite structure. Conversely, the structure of $Ce_{0.9}K_{0.1}CrO_3$ was not maintained after repeated TPC tests, as was previously found for $CeCrO_3$, from which $Ce_{0.9}K_{0.1}CrO_3$ was derived (Palmisano, 2005).

It was not possible to further improve the performance of $TbCrO_3$ or $PrCrO_3$. However, the difference between the peak temperatures of $Ce_{0.5}Pr_{0.3}La_{0.2}CrO_3$ and $PrCrO_3$ was only 8°C. $Ce_{0.5}Pr_{0.3}La_{0.2}CrO_3$ is the most preferable catalytic formulation for industrial application because activity similar to $PrCrO_3$ was achieved with a much smaller quantity of Pr or by employing an even cheaper element such as Ce (www.chemicool.com).

Temperature-programmed desorption (TPD) of oxygen has allowed us to ascertain that the superior activity of $PrCrO_3$ and $Ce_{0.5}Pr_{0.3}La_{0.2}CrO_3$ is related to their higher concentration of weakly chemisorbed suprafacial oxygen species with respect to the other catalytic formulations, such as CeO_2, in the temperature range of interest for soot oxidation purposes (Figure 5).

Figure 6 shows the complete TPC plots for the most promising catalysts of the present study ($TbCrO_3$, $PrCrO_3$, $CeCrO_3$ and $Ce_{0.5}Pr_{0.3}La_{0.2}CrO_3$), for the reference "starting point" catalyst ($LaCrO_3$) and for the non-catalytic combustion of carbon. According to these data, the catalysts showed TPC combustion temperatures significantly lower than 620°C (peak temperature for non-catalytic combustion), especially $PrCrO_3$ and $TbCrO_3$ (peak temperatures of 392°C and 382°C, respectively).

Similar activation energy values were calculated for the various prepared perovskites by the Ozawa method. The perovskite activation energy values (120-145 kJ/mol) were significantly lower than the activation energy of non-catalytic combustion (163 KJ/mol). The Ozawa method is used to report on $Ce_{0.5}Pr_{0.3}La_{0.2}CrO_3$, whose calculated average activation energy was 123.5 kJ/mol, in Figure 7. If an Arrhenius-type kinetics expression is considered, this occurrence boosts the pre-exponential kinetic constant (i.e., the frequency factor) without affecting the activation energy. As a first approximation, the pre-exponential kinetic constant is influenced by the nature of each single oxygen species and not by its concentration.

A comparison with reference catalysts for commercial applications such as Pt/CeO_2 on Al_2O_3 denotes that the peak temperature reached with the $Ce_{0.5}Pr_{0.3}La_{0.2}CrO_3$ catalyst presented in this work is approximately 50°C lower than with Pt-based catalysts tested in similar GHSV, oxygen

concentration and soot/catalyst ratio conditions, but in the presence of 750 ppm of NO (Ivanova et al. 2009), which is decisive in soot oxidation through the NO_2-mediated mechanism promoted by Pt oxidation of NO to NO_2.

3.3 Full-scale tests on a $Ce_{0.5}Pr_{0.3}La_{0.2}CrO_3$-layered trap

The catalyst based on $Ce_{0.5}Pr_{0.3}La_{0.2}CrO_3$ was selected to be deposited on a wall-flow monolith due to the aforementioned considerations concerning the catalyst's activity, stability and cost. Figure 8 compares the results of the induced-regeneration runs obtained with a $Ce_{0.5}Pr_{0.3}La_{0.2}CrO_3$-catalyzed (b) and a non-catalyzed (a) cordierite wall-flow monolith. A major difference between the two traps lies in the degree of completeness of the regeneration process, which is denoted by the decrease of the pressure drop during the regeneration itself. A further index of the high combustion rate induced by the catalyst is the remarkable difference between the upstream (lower) and the downstream (higher) temperatures, a direct consequence of the heat released from soot combustion. As a consequence, by significantly lowering the soot combustion temperature, it is possible to save a significant amount of fuel at filter regeneration, thereby reducing the operating costs.

These results pave the way towards the development of new catalysts capable of maximizing the concentration of suprafacial reactive oxygen species in the temperature range of interest for diesel engine exhaust gases (150-380°C).

Conclusions

The experimental activities performed in our laboratories suggest the possibility of using new rare earth based perovskites as catalysts for catalyzed wall-flow filters. The catalytic activity tests suggest that the $Ce_{0,5}Pr_{0,3}La_{0,2}CrO_3$ perovskite is the most promising catalyst. The fact that praseodymium is an unconventional element for catalysis might cause some concern and lead to worry about the cost. In this context, it is worth mentioning that Pr is a side product of Ce

production. The extensive use of Ce in catalysis has led to a large accumulation of unused Pr in the US. As a consequence, the cost of praseodymium has significantly decreased in recent years and it is currently much less expensive than noble metals, e. g., Pt and Pd (www.chemicool.com).

The wall-flow ceramic filter catalyzed with $Ce_{0,5}Pr_{0,3}La_{0,2}CrO_3$ obtained through *in-situ* SCS confirmed the promising results obtained with the powder catalyst, due to the fuel saving that a fast and complete filter regeneration entails.

References:

Aneggi E., de Leitenburg C., Trovarelli A. (2012a) On the role of lattice/surface oxygen in ceria–zirconia catalysts for diesel soot combustion, *Cat. Tod.*, **181**, 108.

Aneggi E., de Leitenburg C., Llorca J., Trovarelli A. (2012b) Higher activity of Diesel soot oxidation over polycrystalline ceria and ceria–zirconia solid solutions from more reactive surface planes, *Cat. Tod.*, **197(1)**, 119.

Atribak I., Bueno-López A., and García-García A. (2008). Combined removal of diesel soot particulates and NO_x over CeO_2–ZrO_2 mixed oxides, *J. Catal.*, **259**, 123.

Badini C., Saracco G., Russo N., and Specchia V. (2000). A screening study on the activation energy of vanadate-based catalysts for diesel soot combustion, *Catal. Lett.*, **69**, 207.

Bensaid S., Marchisio D.L. and Fino D. (2010) Numerical simulation of soot filtration and combustion within diesel particulate filters, *Chem. Eng. Sci.*, **65**, 357.

Bensaid S., Marchisio D.L., Russo N., Fino D. (2009a) Experimental investigation of soot deposition in diesel particulate filters, *Cat. Tod.* **147S**, S295.

Bensaid S., Marchisio D.L., Fino D., Saracco G., Specchia V. (2009b) Modeling of diesel particulate filtration in wall-flow traps, *Chem. Eng. J.*, **154:1-3**, 211.

Bensaid S., and Russo N. (2011). Low temperature DPF regeneration by delafossite catalysts, *Catal. Today*, **176**, 417.

Caroca J.C., Millo F., Vezza D., Vlachos T., De Filippo A., Bensaid S., Russo N. and Fino D. (2011) Detailed Investigation on Soot Particle Size Distribution during DPF Regeneration, using Standard and Bio-Diesel Fuels, *Ind. Eng. Chem. Res.*, **50(5)**, 2650.

Civera A., Pavese M., Saracco G., and Specchia V. (2003). Combustion synthesis of perovskite-type catalysts for natural gas combustion, *Catal. Today*, **83**, 19.

Darcy P., Costa P., Mellottée H., Trichard J. M., and Djéga-Mariadassou G. (2007). Kinetics of catalyzed and non-catalyzed oxidation of soot from a diesel engine, *Catal. Today*, **119**, 252.

Fino D., Russo N., Saracco G., and Specchia V. (2003a). The role of suprafacial oxygen in some perovskites for the catalytic combustion of soot, *J. Catal.* **217**(2), 367.

Fino D., Fino P., Saracco G., Specchia V. (2003b) Innovative means for the catalytic regeneration of particulate traps for diesel exhaust cleaning. Chemical Engineering Science 58 (3–6), 951.

Fino D. and Specchia V. (2004) Compositional and structural optimal design of a nanostructured diesel-soot combustion catalyst for a fast-regenerating trap, Chem. Eng. Sci. 59, 4825.

Krishna K., Bueno-López A., Makkee M., Moulijn J.A. (2007) Potential rare-earth modified CeO_2 catalysts for soot oxidation part II: Characterisation and catalytic activity with $NO+O_2$, *Appl. Catal. B*, **75**, 201.

Kumar P.A., Tanwar M.D., Bensaid S., Russo N., Fino D. (2012) Soot Combustion Improvement in Diesel Particulate Filters Catalyzed with Ceria Nanofibers, *Chem. eng. J.*, **207-208**, 258.

Ivanova A.S., Litvak G.S., Mokrinskii V.V., Plyasova L.M., Zaikovskii V.I., Kaichev V.V. and Noskov A.S. (2009) The influence of the active component and support nature, gas mixture composition on physicochemical and catalytic properties of catalysts for soot oxidation, *J. Mol. Catal. A: Chem.*, **310**, 101.

Merzahanov, A. G. (1996). Combustion Process that Synthesize Materials, *J. of Mat. Proc. Techn.*, **56**, 222.

Neumann H.G., (2002) Health risk of combustion products: toxicological considerations, *Chemosphere*, **42**, 473.

Ozawa, T. (1970). Kinetic analysis of derivative curves in thermal analysis, *J. Therm. Anal.*, **2**, 301.

Ozawa, T. (1975). Critical investigation of methods for kinetic analysis of thermo-analytical data, *J. Therm. Anal.*, **7**, 601.

Palmisano P., Biamino S., Fino P., Badini C. (2005), Catalytic activity of rare earth perovskites towards soot combustion, Proceedings of the European Combustion Meeting - ECM 2005, Louvain-la-Neuve, Belgium, 3-6 April 2005.

Pontikakis G. N., Koltsakis G. C., and Stamatelos A. M. (2001). Dynamic filtration modeling in foam filters for diesel exhaust, *Chem. Eng. Comm.*, **188**, 21.

Pope III C.A., Burnett R.T., Thurston G.D., Thun M.J., Calle E.E., Krewski D. and Godleski J.J. (2004) Cardiovascular mortality and long-term exposure to particulate air pollution, *Circulation*, **109**, 71.

Russo N., Fino D., Saracco G., and Specchia V. (2005). Studies on the redox properties of chromite perovskite catalysts for soot combustion, *J. Catal.*, **229**, 459.

Ye S.H., Zhou W., Song J., Peng B.C., Yuan D., Lu Y.M. and Qi P.P. (1999) Toxicity and health effects of vehicle emissions in Shanghai, *Atm. Env.*, **34**, 419.

Table 1. Specific surface area of the selected perovskite catalysts

Perovskite Catalyst	Surface area
$CeCrO_3$	32.9 m^2/g
$PrCrO_3$	20.5 m^2/g
$TbCrO_3$	19.8 m^2/g
$Ce_{0.5}Pr_{0.3}La_{0.2}CrO_3$	22.1 m^2/g

List of Figures

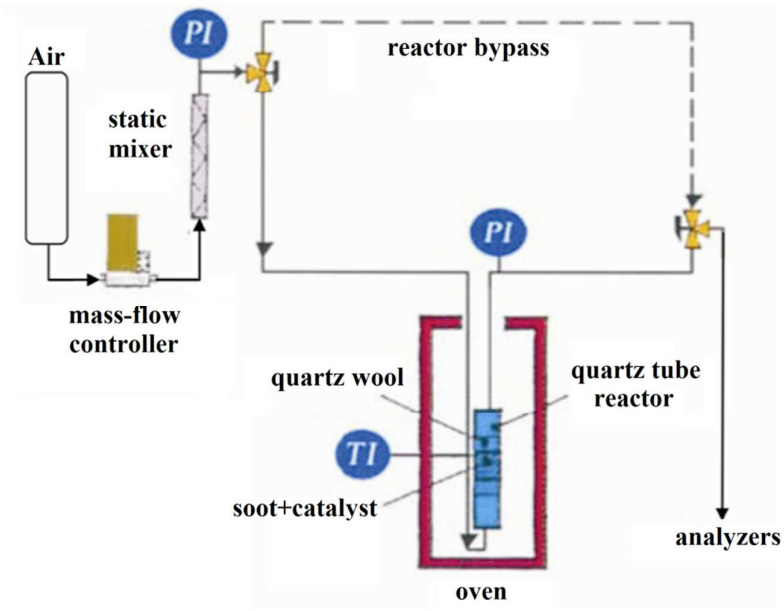

Figure 1

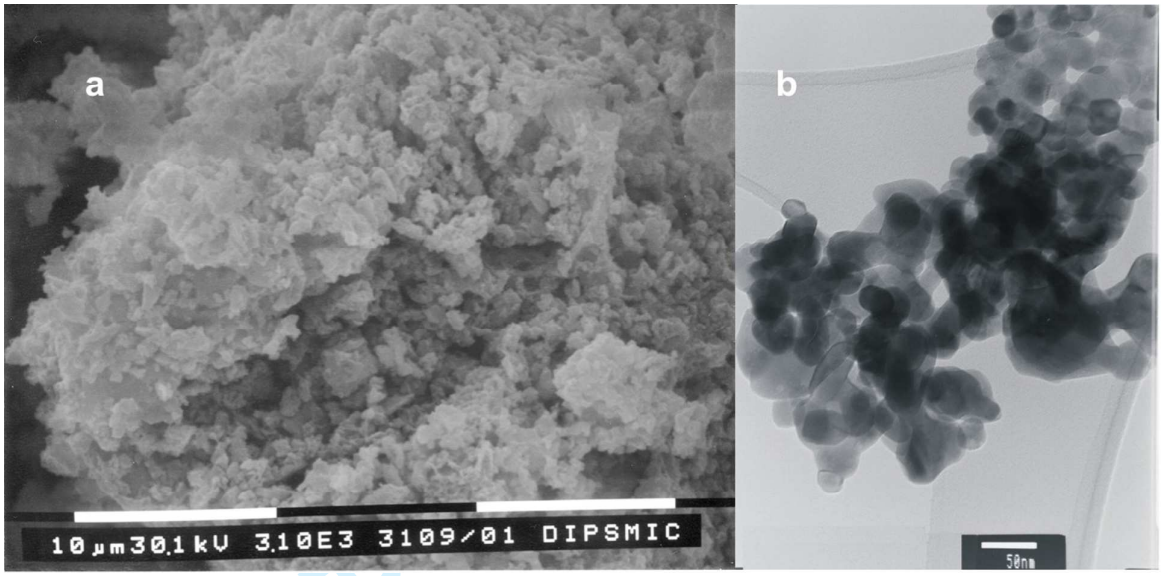

Figure 2

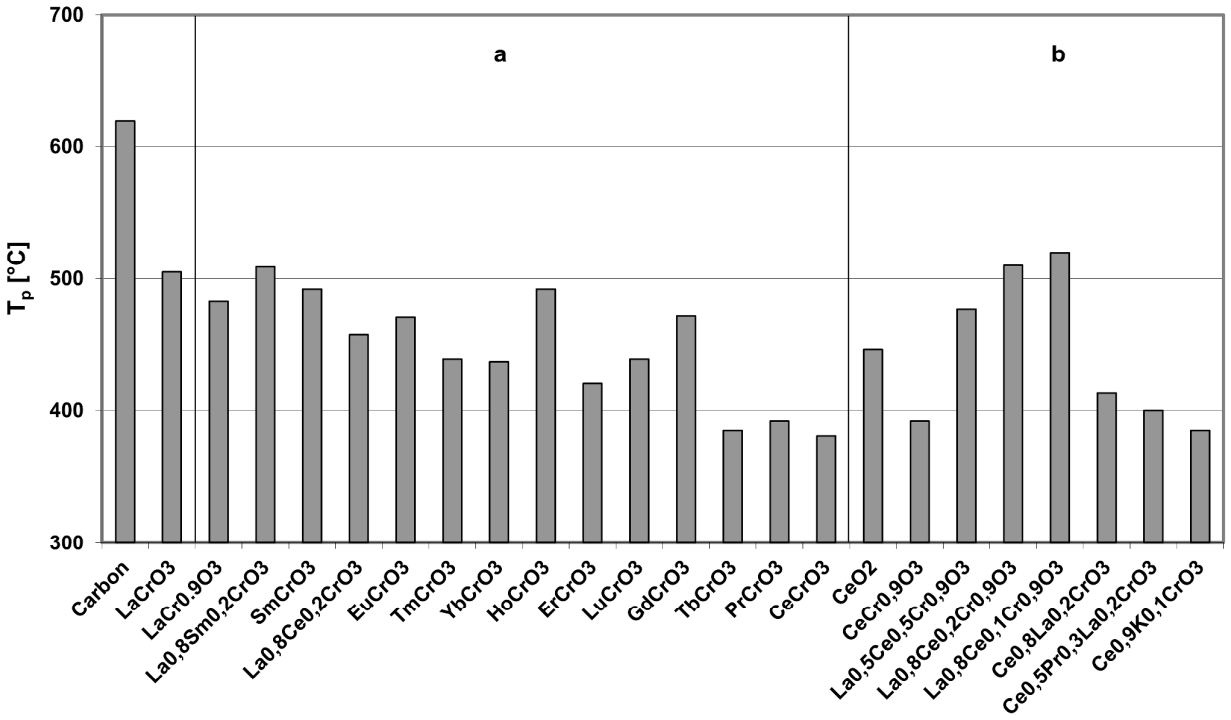

Figure 3

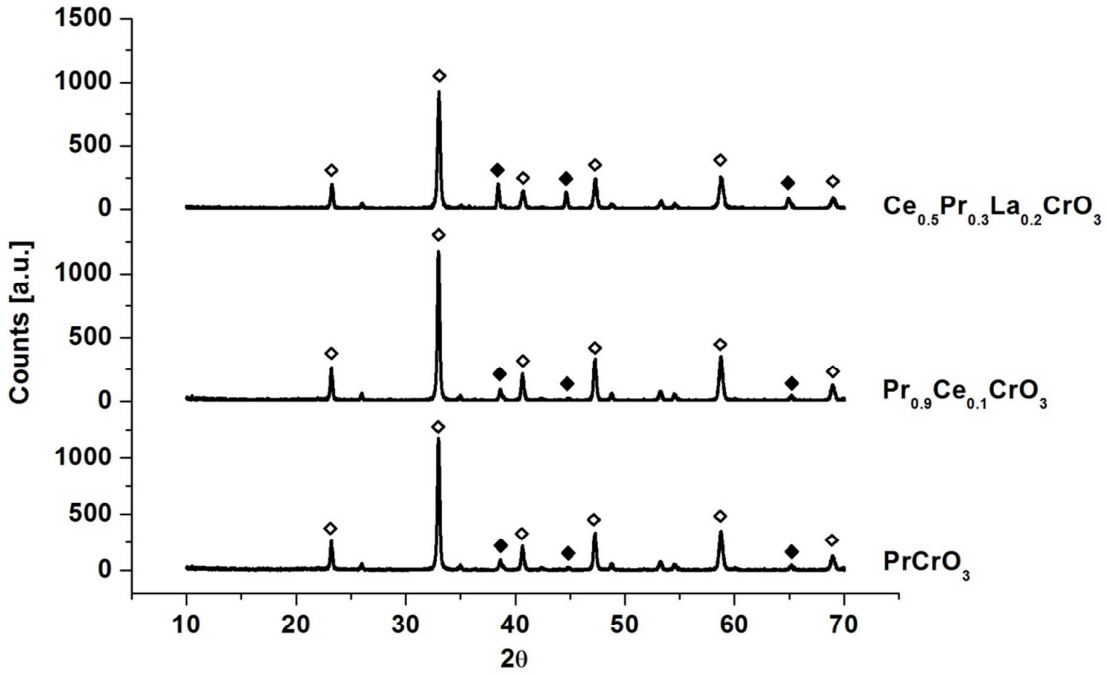

Figure 4

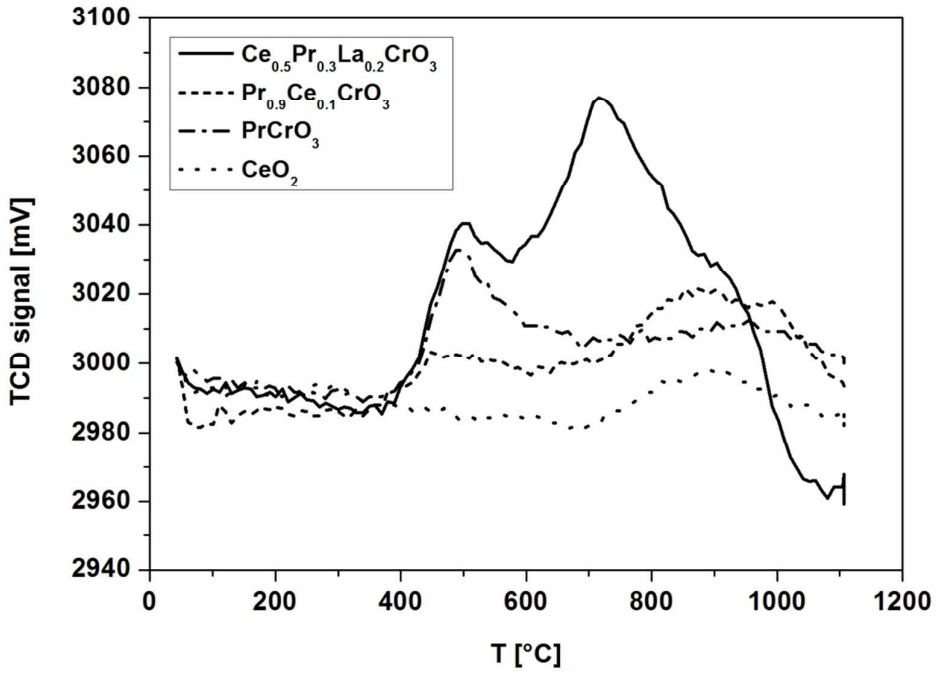

Figure 5

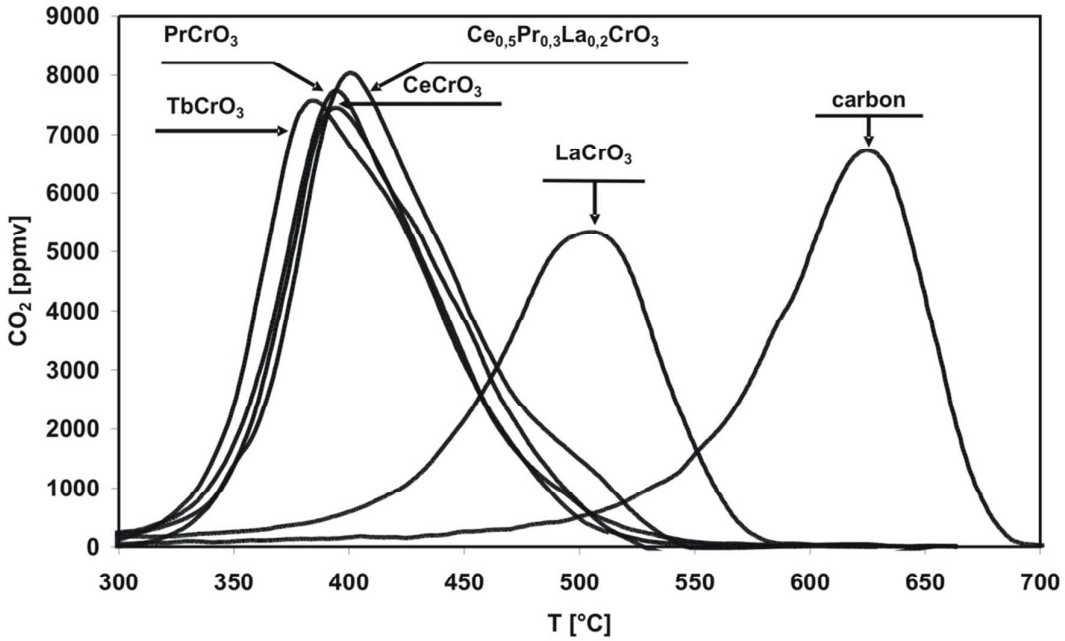

Figure 6

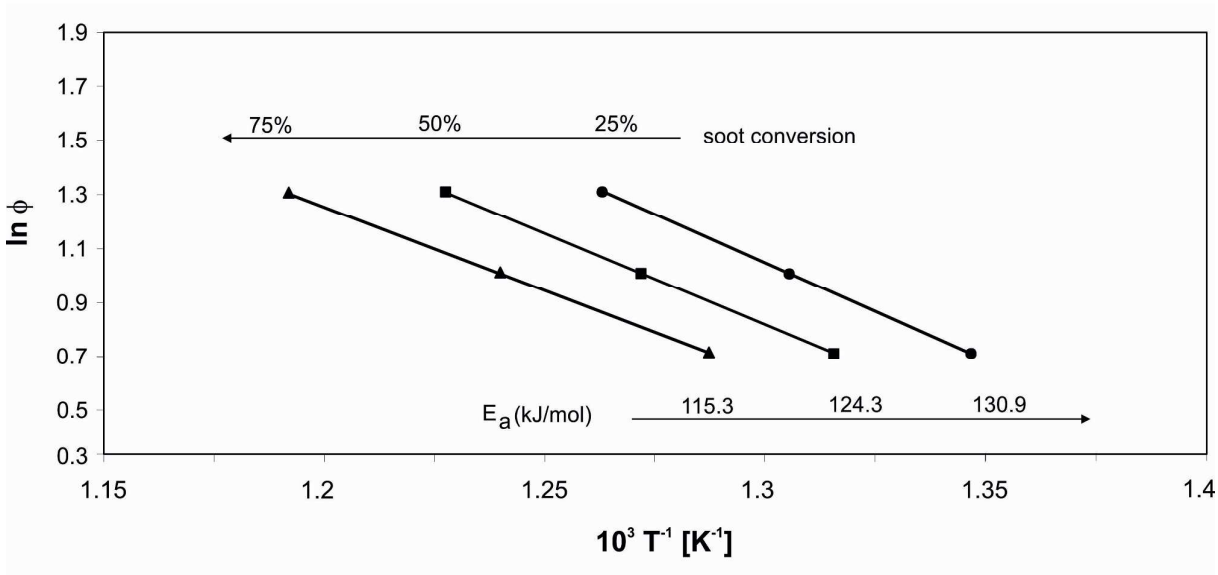

Figure 7

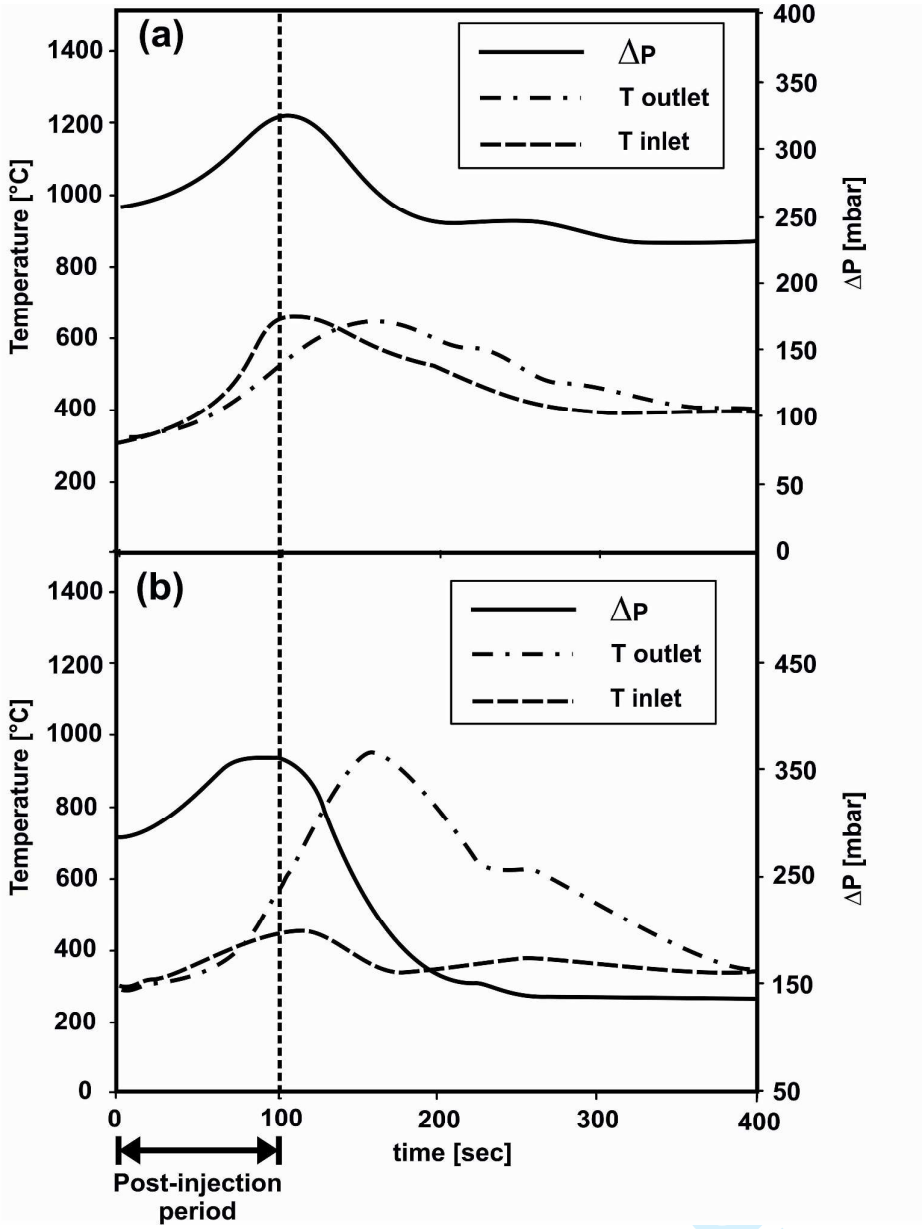
(a)
ΔP
T outlet
T inlet
Temperature [°C]
ΔP [mbar]
(b)
ΔP
T outlet
T inlet
Temperature [°C]
ΔP [mbar]
time [sec]
Post-injection period

Figure 8